

ENGINEERING PERSPECTIVE

CONTENTS

Research Articles

Page Number

Turan Alp ARSLAN, Faruk Emre AYSAL, İbrahim ÇELİK, Hüseyin BAYRAKÇEKEN, Tuğçe Nur ÖZTÜRK

Quarter Car Active Suspension System Control Using Fuzzy Controller 33-39

Ahmet UYUMAZ, Şenol GÜZEL, Abdullah KÖSE, Sinan SATILMIŞ, Burak POLAT, Oğuzhan KARAKAŞ, Yiğitcan KÜÇÜKÇELEN

Autonomous Feed Pushing Robot Design and Manufacturing 40-45

Mehmet Can KATMER, Adnan AKKURT, Tolga KOCAKULAK

Investigation of Natural Frequency Values of Composite Cover Design with Different Laying Angles 46-51

ENGINEERING PERSPECTIVE

Volume: 2

Issue: 4

31 December 2022

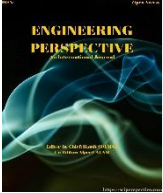
ENGINEERING PERSPECTIVE

An International Journal

Volume: 2

Issue: 4

31 December 2022



Quarter Car Active Suspension System Control Using Fuzzy Controller

Turan Alp Arslan¹, Faruk Emre Aysal^{2*}, İbrahim Çelik², Hüseyin Bayrakçeken¹, Tuğçe Nur Öztürk²

¹ Automotive Engineering Department, Faculty of Technology, Afyon Kocatepe University, Afyonkarahisar, 03200, Türkiye

² Mechatronics Engineering Engineering, Faculty of Technology, Afyon Kocatepe University, Afyonkarahisar, 03200,

ABSTRACT

The performance of active suspension systems is directly related to the mechanical design and control of the system. The stable operation of the controller improves driving comfort and handling. The quarter car model is frequently used in the analysis of suspension systems due to its simple structure. In this study, Matlab Simulink software was used in the modeling, control and simulation of the quarter car active suspension model. System performance was investigated for four different road profiles with PID and fuzzy logic control methods. Two of the road profiles used are in the form of impact signals consisting of pits and bumps. The other two road profiles are random road disturbances with high frequency. The effects of active and passive suspension systems on driving comfort are compared by taking into account the control methods used. As a result of the study, it has been determined that the fuzzy logic controller gives better results in pulse signals consisting of bumps and pits, and the PID controller gives better results in high-frequency random road disturbances. In addition, with the use of fuzzy logic control method in the active suspension system, a significant decrease in the actuator force has occurred. This result is very interesting in terms of minimizing energy, reducing actuator sizes and reducing costs.

Keywords: Active suspension, Fuzzy logic, Quarter car model, Vehicle dynamics.

History

Received: 23.08.2022

Accepted: 17.11.2022

Author Contacts

*Corresponding Author

e-mail addresses : talparslan@aku.edu.tr, faysal@aku.edu.tr, icelik@aku.edu.tr, bceken@aku.edu.tr, tugcenurozturk06@gmail.com.

Orcid numbers : 0000-0003-3259-4854, 0000-0002-9514-1425, 0000-0002-8857-1910, 0000-0002-1572-4859, 0000-0003-0354-8058

<http://dx.doi.org/10.29228/eng.pers.66798>

1. Introduction

Irregularities on the roads adversely affect the comfort and safety of vehicles. For this reason, suspension systems in various designs have been used in vehicles since the end of the 19th century. Vehicle suspension systems play an important role in reducing the vertical acceleration of the chassis and providing comfortable and safe driving. Today, classical suspension systems consisting of coil springs and damping elements on each wheel are used as standard in passenger vehicles [1,2].

The traditional suspension system used in passenger vehicles consists of three basic components: shock absorber, coil spring and connecting elements. Here, the shock absorber performs the duty of absorbing the shocks originating from the road, and the coil spring performs the task of storing the energy coming to the chassis. The connecting elements provide the connection between the wheel hub and the suspension elements and the connection between the chassis and the suspension. Traditionally, systems with constant damping and spring coefficient, known as passive suspension systems, are used in

vehicles. Suspension systems whose damping properties or vertical acceleration ability can be adjusted by a control element are known as active suspension systems. In order to improve driving comfort and safety, researchers carry out many studies on systems known as active suspension systems [3-9].

Various approaches are discussed as a control element in active suspension systems. It is a common approach to use Magneto-Rheological (MR) fluid instead of the hydraulic fluid used in the shock absorber system. By using MR fluid, hydraulic fluid viscosity can be changed by a control current. Thus, the damping rate of the shock absorber can be actively controlled. This approach is accepted as a semi-active suspension system in the literature [10-13]. Another widely considered approach is to add a linear actuator to the conventional suspension system. Thanks to the additional force provided by this actuator, the vertical acceleration in the suspension system becomes controllable. This form of suspension system is known as active suspension [14-19].

Stable control of active and semi-active suspension systems is an important problem for the widespread use of these systems. For this

reason, many different control approaches are considered by researchers. Various methods such as optimal control theory, feedback control system, robust, LQR, PID, fuzzy logic are used for the control of the active suspension system [20-27].

Fuzzy logic is accepted as an important solution method for dynamic systems that want to be controlled adaptively. Therefore, there are many studies on the development of control algorithms using fuzzy logic in active suspension systems. Studies show that fuzzy logic controllers provide successful results for active suspension systems. However, it is seen that the majority of the studies carried out are on simulation and mathematical modeling [28-37]. Therefore, the improvement of the control approaches by comparing them with different methods and making real applications in the following stages is still a topic of current study.

In this study, active suspension system control was realized by using PID and fuzzy logic control methods. MATLAB Simulink software was used for modelling, control and simulation studies of the quarter car active suspension system. Passive and active suspension system results were obtained for four different road profiles. The displacement, velocity, acceleration and actuator controls of the vehicle body were examined and the superiority of PID and fuzzy logic control methods over each other was investigated. The effects of the control structures created in the simulation results on the driving comfort and control force are discussed.

2. Quarter Car Active Suspension Model

The quarter car model has a simple and easy-to-understand structure. It is frequently used in suspension system design and simulation because it reflects the important features of the full car. The passive quarter car model has two main masses, spring and unsprung, two springs and a damper. This system is activated with the actuator added between the body and the axle. Actuators, which generally consist of electro-hydraulic elements, provide the control of the system by generating forces in both directions. With the system control, the effects of vibrations caused by road disturbances on the vehicle body and passengers are reduced [38, 39]. The quarter car active suspension model with 2 degrees of freedom is shown in Figure 1.

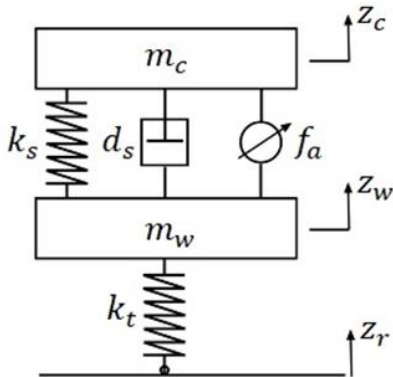


Figure 1. Quarter car active suspension model

In this model, the spring mass m_c , which corresponds to one fourth of the vehicle body mass, is represented by the unsprung mass of the axle and wheel components m_w , the passive components of the spring and damper coefficients k_s and d_s , respectively, the tire stiffness k_t and the control force produced by the actuator f_a .

In addition, the displacement of the spring and unsprung masses are indicated by z_c and z_w , respectively, and the road profile affecting the unsprung mass is indicated by z_r . The constant parameters of the quarter car active suspension system are shown in Table 1.

Table 1. Parameters of active suspension system

Parameters	Values
m_c (kg)	300
m_w (kg)	50
k_s (N/m)	18000
k_t (N/m)	190000
d_s (N-s/m)	2000

The linear equations of motion for the spring and unsprung masses of the system are defined using Newton's second law as follows:

$$m_w \ddot{z}_w = k_t(z_r - z_w) - k_s(z_w - z_c) - d_s(\dot{z}_w - \dot{z}_c) - f_a \quad (1)$$

$$m_c \ddot{z}_c = k_s(z_w - z_c) + d_s(\dot{z}_w - \dot{z}_c) + f_a \quad (2)$$

In order to develop the state space model of the system x_1, x_2, x_3 and x_4 parameters are accepted as state variables. Here x_1 represents the displacement of the unsprung mass, x_2 the velocity of the unsprung mass, x_3 the displacement of the spring mass and x_4 the velocity of the spring mass. Quarter car active suspension model equations of motion are converted into state space model with the help of the following expressions:

$$x_1 = z_w \quad (3)$$

$$x_2 = \dot{z}_w \quad (4)$$

$$x_3 = z_c \quad (5)$$

$$x_4 = \dot{z}_c \quad (6)$$

$$\dot{x}_1 = x_2 \quad (7)$$

$$\dot{x}_2 = \frac{1}{m_w} [k_t z_r - (k_t + k_s)x_1 - d_s x_2 + k_s x_3 + d_s x_4 - f_a] \quad (8)$$

$$\dot{x}_3 = x_4 \quad (9)$$

$$\dot{x}_4 = \frac{1}{m_c} [k_s x_1 + d_s x_2 - k_s x_3 - d_s x_4 + f_a] \quad (10)$$

The state space model used to explain the system dynamics is obtained as follows:

$$\dot{x} = Ax + Bu \quad (11)$$

$$y = Cx \quad (12)$$

$$x = [x_1, x_2, x_3, x_4]^T \quad (13)$$

$$u = [f_a, z_r]^T \quad (14)$$

$$A = \begin{bmatrix} 0 & 1 & 0 & 0 \\ -\frac{k_t + k_s}{m_w} & -\frac{d_s}{m_w} & \frac{k_s}{m_w} & \frac{d_s}{m_w} \\ 0 & 0 & 0 & 1 \\ \frac{k_s}{m_c} & \frac{d_s}{m_c} & -\frac{k_s}{m_c} & -\frac{d_s}{m_c} \end{bmatrix} \quad (15)$$

$$B = \begin{bmatrix} 0 & 0 \\ 1 & k_t \\ \frac{m_w}{m_c} & \frac{m_w}{m_c} \\ 0 & 0 \\ 1 & 0 \\ \frac{1}{m_c} & 0 \end{bmatrix} \quad (16)$$

$$C = [0 \quad 0 \quad 1 \quad 0] \quad (17)$$

3. Controller Design

In the study, two types of controllers were used to control the quarter car active suspension. These are proportional-integral-derivative (PID) controller and fuzzy logic (FLC) controller.

PID controllers are a very common form of control in control systems due to their simple structure, low number of variables to be adjusted and ease of physical implementation. This controller, which has three parameters as proportional (P), integral (I) and derivative (D), determines the amount of error by comparing the signal coming from the system output with the reference signal. Depending on the set variables, the controller effect is sent to the output, thus minimizing the error. The mathematical formula of the PID controller working with continuous feedback is as follows:

$$u(t) = K_p e(t) + K_i \int_0^t e(t) dt + K_d \frac{d}{dt} e(t) \quad (18)$$

Here K_p is the proportional gain, K_i integral gain, K_d derivative gain, $e(t)$ is the difference between the set point and the measured process variable at the relevant time, and $u(t)$ is the controller effect on the process at the relevant time. PID controller performance is directly based on accurate determination of controller gains [40].

The MATLAB Simulink model of quarter car active suspension system controlled by a PID controller is shown in Figure 2. In this study, the displacement of the spring mass z_c , which corresponds to one fourth of the vehicle body mass, is fed back to the system. The road profile z_r acting on the unsprung mass is accepted as the reference signal. The PID controller output, on the other hand, affects the system again as the activation force f_a .

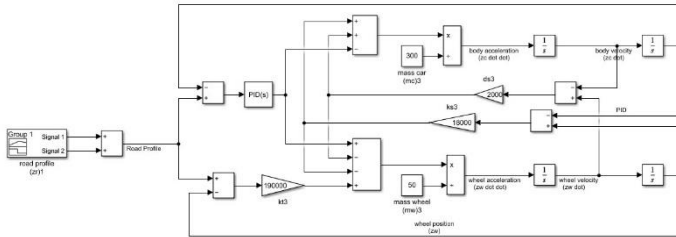


Figure 2. Simulink model of active suspension system using PID controller

Fuzzy logic basically tries to imitate the decision-making style that takes place in the human brain. In this method, where it is accepted that the decisions are not final, quantitative and binary, the answers may be in shades of gray, not black and white [41]. The fuzzy logic controller consists of three parts: the fuzzifier, the inference unit and the defuzzifier. The fuzzifier is responsible for converting the input values to fuzzy values, the inference unit is responsible for processing the data and calculating the controller outputs, and the defuzzifier is responsible for converting the outputs to real

numbers [42]. In fuzzy logic applications, it is of great importance that the input-output parameters, membership functions and control rules are set correctly by the expert.

The vertical displacement and velocity of the system are fuzzy logic inputs in this study. These input parameters can also be defined as error and change of error. The output parameter of the controller is the control force desired to be effected on the system with the help of the actuator. The fuzzy logic input parameters are expressed as follows:

$$fuzzy_{input1} = z_c - z_r \quad (15)$$

$$fuzzy_{input2} = \dot{z}_c - \dot{z}_r \quad (16)$$

In Figures 3 and 4, membership functions of fuzzy logic input parameters are seen, and in Figure 5, membership functions of the output parameter are seen. Inputs and output have five trapezoidal membership functions. In these figures, NB, NS, Z, PS, and PB denote negative big, negative small, zero, positive small, and positive big, respectively.

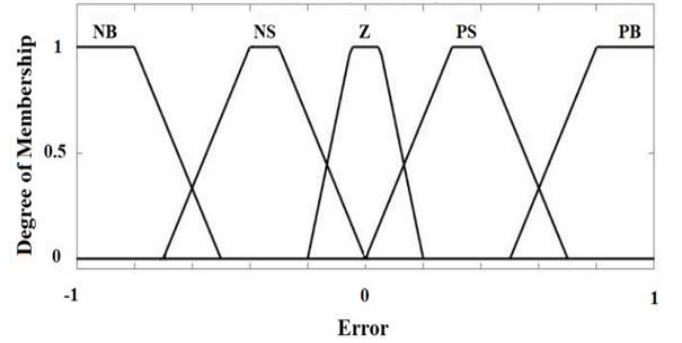


Figure 3. Membership functions for error

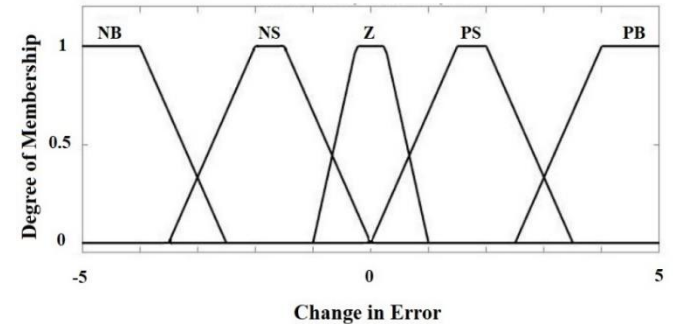


Figure 4. Membership functions for change in error

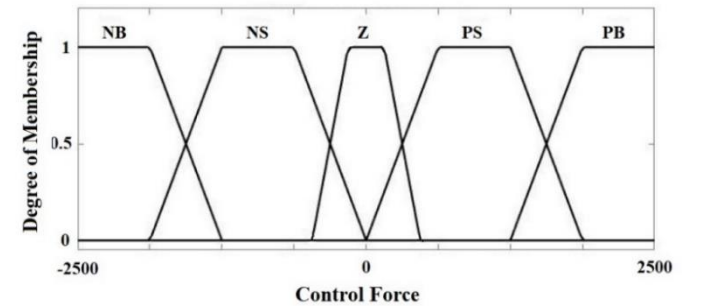


Figure 5. Membership functions for control force

The rule base created for the quarter car active suspension system is created based on the expert's knowledge and experience, as in other applications. The fuzzy logic rule matrix of the study, in which the classical "Mamdani" approach was used for the rule base, is shown in Table 2. There are 25 control rules in total in the created rule base.

Table 2. Fuzzy logic rule matrix

e/Ce	NB	NS	Z	PS	PB
NB	NB	NB	NS	NS	Z
NS	NB	NS	NS	Z	PS
Z	NS	NS	Z	PS	PS
PS	NS	Z	PS	PS	PB
PB	Z	PS	PS	PB	PB

NB: Negative Big; NS: Negative Small; Z: Zero; PS: Positive Small; PB: Positive Big; e: Error; Ce: Change in Error

Figure 6 shows the fuzzy logic surface plot for the input and output parameters, and the MATLAB Simulink model of the quarter car active suspension controlled by a fuzzy logic controller is shown in Figure 7.

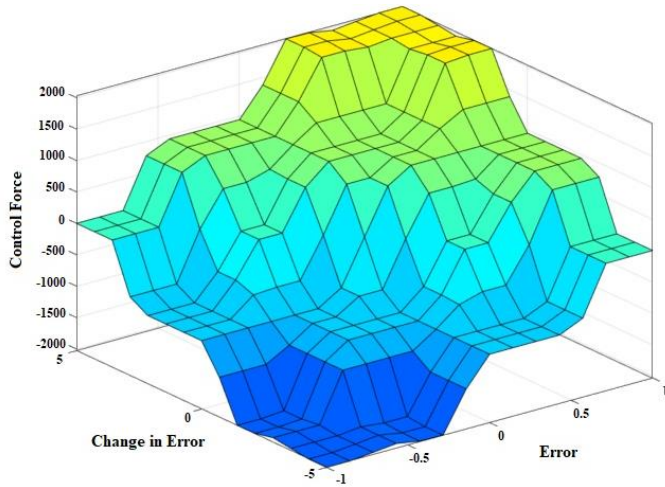


Figure 6. Fuzzy logic surface plot

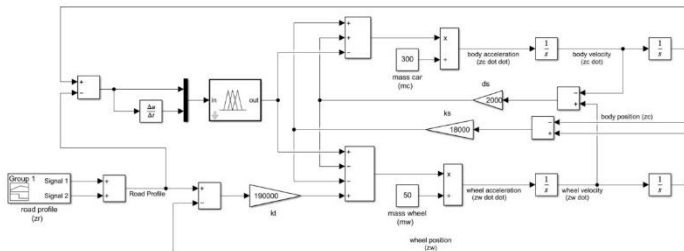


Figure 7. Simulink model of active suspension system using fuzzy logic controller

4. Simulation Results

In this study, active suspension quarter car suspension system control was carried out with two different controllers, PID and FLC. MATLAB Simulink software was used in the modeling, control and simulation of the system. The effects of the control structures created in the simulation results on the driving comfort and control force were

investigated. The performance of the simulation models was investigated for four different road profiles. In order to best observe the active suspension characteristics and controller effects, two of the road profiles were created from potholes and bumps, while the other two were created from high frequency random road disturbances. Interesting results emerged when the displacement amount of the spring mass z_c , which represents the vehicle body for all road profiles, was analysed. The variation of the spring mass displacement z_c with time for the first road profile simulating a bump and then a pit is shown in Figure 8.

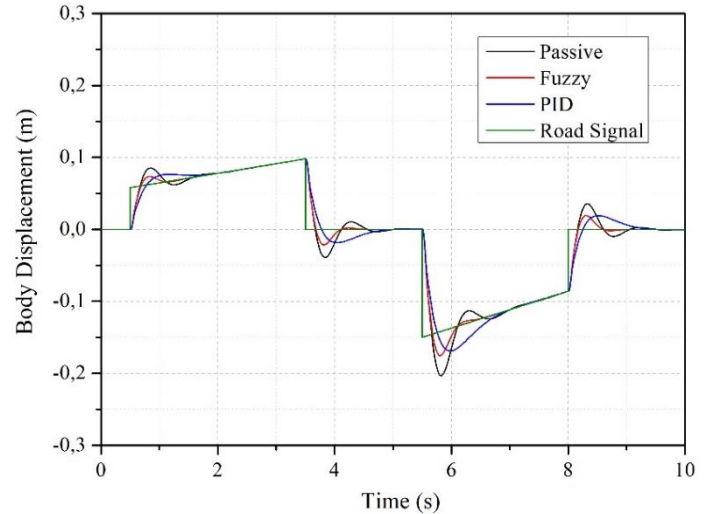


Figure 8. Body displacement for first road profile

When the figure is examined, it is clearly seen that the control application with PID and fuzzy logic controller in the active suspension system provides an improvement in driving comfort. For the first road profile, it can be said that fuzzy logic control gives better results than PID controller with fast rise time and fast settling time. In the PID controller, the amount of overshoot is close to that of fuzzy logic, but the system becomes stable in a longer time. When the passive suspension performance is examined, it is seen that the settling time and the overshoot amount of the system are quite high. Both control structures have reduced the amount of body displacement, amplitude and frequency compared to the passive suspension.

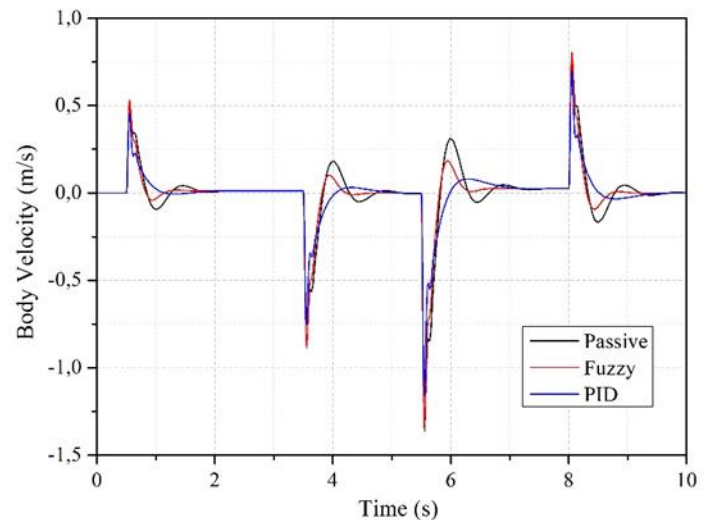


Figure 9. Body velocity for first road profile

It is clearly seen that the fuzzy logic and PID control signal amplitude is less than half of the passive suspension signal. The variation of spring mass velocity \dot{z}_c and spring mass acceleration \ddot{z}_c for the first road profile with time is shown in Figure 9 and Figure 10, respectively.

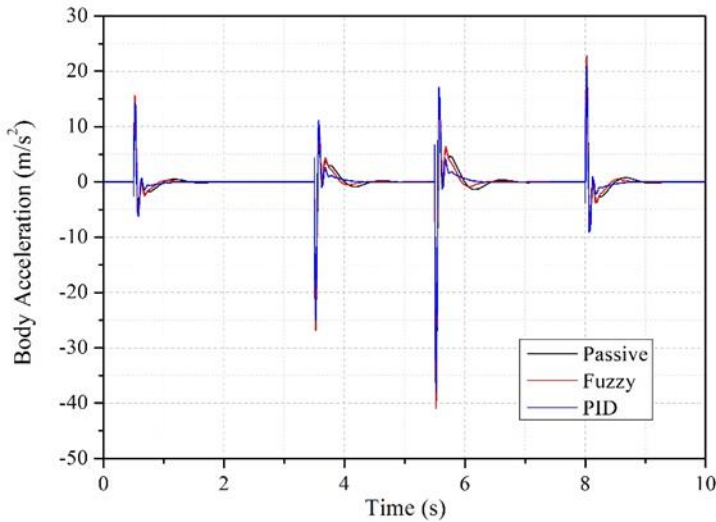


Figure 10. Body acceleration for first road profile

When the body velocity and acceleration results are examined, it is seen that the maximum values for all models are close to each other. However, as in the amount of body displacement, the active suspension system controlled by fuzzy logic has become stable in a shorter time. This indicates an improvement in driving comfort. The time-dependent variation of the control force f_a obtained as a result of the simulation carried out for the first road profile is shown in Figure 11.

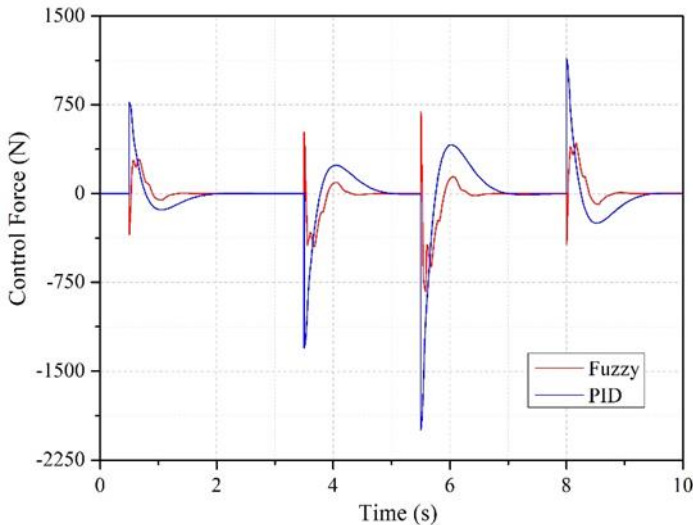


Figure 11. Control force for first road profile

With the use of fuzzy logic controller, decreases were observed in the active suspension control force compared to the PID controller. This will enable the use of smaller and lower cost actuators with fuzzy logic control. Minimizing the amount of energy used, reducing the size of the actuator element to be used on a moving vehicle and reducing costs are

as important as improving driving comfort. While the system controlled by PID controller needs an actuator force of 1850 N, this force has decreased to 760 N with fuzzy logic control. The variations of the vehicle body displacement z_c for other simulated road conditions with time are shown in Figures 12, 13 and 14.

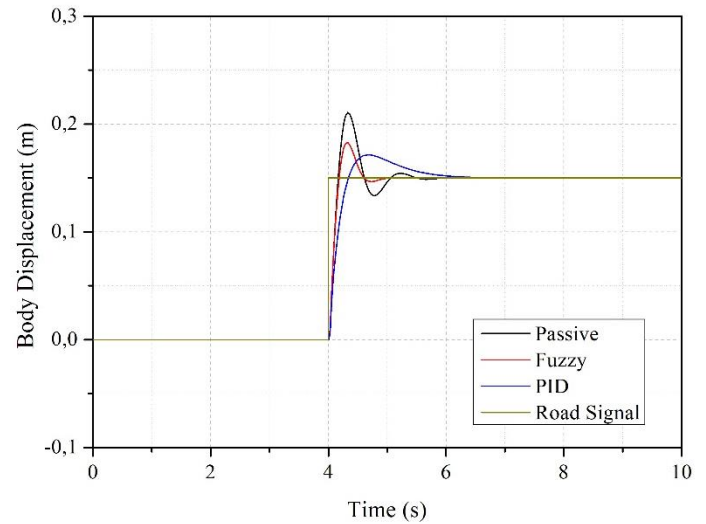


Figure 12. Body displacement for second road profile

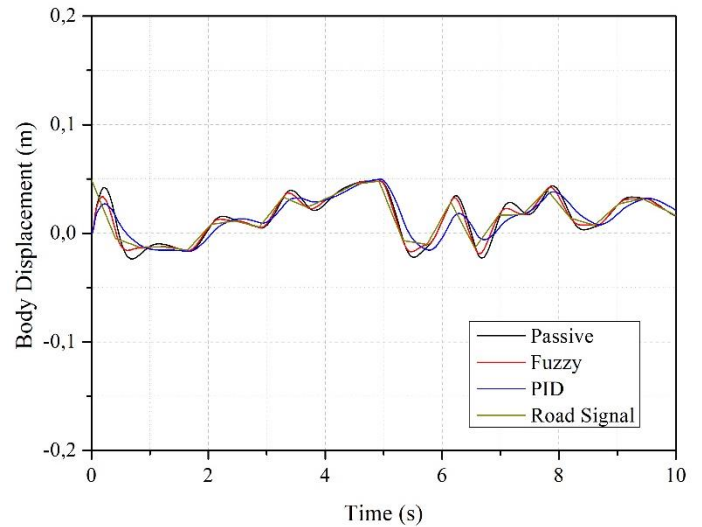


Figure 13. Body displacement for third road profile

In the second road profile with a bump signal, it is seen that the displacement amount for the fuzzy logic-controlled system is slightly higher than the PID controlled system. However, as in the first road profile, a more stable body movement occurred with rapid rise and settling times. Although the displacement is low in the PID controlled system, it is not acceptable for the signal setting time to take about 1 second. In addition, both PID and fuzzy logic results will provide better driving comfort compared to the passive suspension system. High amplitude and oscillation in the passive suspension system signal will adversely affect driving comfort. When the results for the third and fourth road profiles where random disturbances are defined are examined, it is seen that the active suspension system using PID controller provides better results with low body displacement. While the fuzzy logic controller

stands out in bumps and potholes that can be described as pulse signals, the PID controller has an advantage in continuous road disturbances with high frequency.

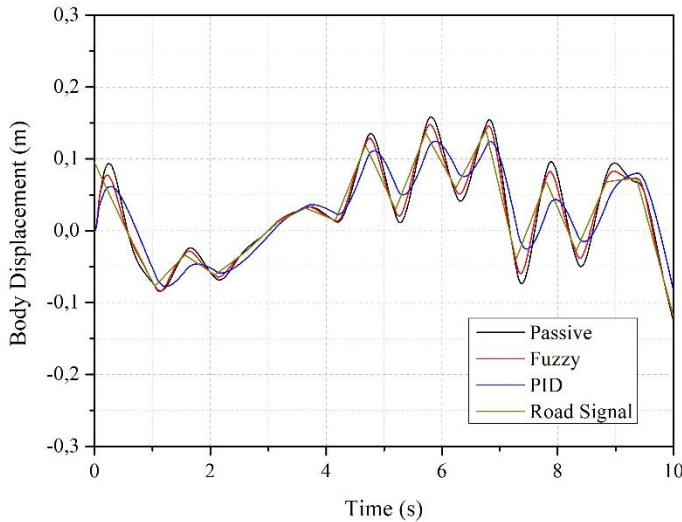


Figure 14. Body displacement for fourth road profile

5. Conclusion

In this study, PID and fuzzy logic control methods are used for active suspension control. MATLAB Simulink software was used in the modeling, control and simulation of the quarter car active suspension system. The simulation results for four different road profiles were compared with each other and with the passive suspension system. Compared to the passive suspension system, it has been found that both methods effectively stabilize the suspension system and provide significant improvements in driving comfort. As a result of the study, it has been confirmed that both PID and fuzzy logic control give successful results in active suspension system control. The fuzzy logic controller has come to the forefront with its low oscillation, short rise and settling time in road disturbances that can be defined as an impact signal consisting of pits and bumps. In high frequency random path disturbances, the system with PID controller has an advantage with its low displacement amount. With the use of fuzzy logic control, a 59% decrease in actuator control force has occurred. This value is very interesting in terms of reducing the actuator dimensions, reducing the costs and minimizing the energy used. It is thought that testing different control methods and different disturbance inputs on half or full vehicle models will be beneficial for the development of active suspension systems.

Nomenclature

C_e	change in error
e	error
d_s	suspension damping coefficient (N-s/m)
f_a	actuation force (N)
FLC	Fuzzy Logic Controller
k_s	suspension stiffness (N/m)
k_t	tyre stiffness (N/m)
K_d	derivative gain
K_i	integral gain
K_p	proportional gain
LQR	Linear Quadratic Regulator

m_c	sprung mass (kg)
m_w	unsprung mass (kg)
MR	Magneto-Rheological
PID	Proportional Integral Derivative
u	controller effect
z_c	displacement of sprung mass(m)
z_r	road profile (m)
z_w	displacement of unsprung mass (m)

Conflict of Interest Statement

The authors declare that there is no conflict of interest in the study.

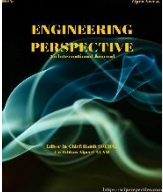
CRedit Author Statement

Turan Alp Arslan: Conceptualization, Writing-original draft, Validation, **Faruk Emre Aysal:** Conceptualization, Writing-original draft, Supervision, **İbrahim Çelik:** Conceptualization, Formal analysis, **Hüseyin Bayrakçeken:** Conceptualization, Supervision, **Tuğçe Nur Öztürk:** Formal analysis

References

- Samadi, F., and Moghadam-Fard, H. (2015). Active suspension system control using adaptive neuro fuzzy (anfis) controller. *International Journal of Engineering*, 28(3), 396-401.
- Altun, Y. (2017). Çeyrek taşıt aktif süspansiyon sistemi için LQR ve LQI denetleyicilerinin karşılaştırılması. *Gazi Üniversitesi Fen Bilimleri Dergisi Part C: Tasarım ve Teknoloji*, 5(3), 61-70.
- Basari, A. A., and Saat, M. S. M. (2007). Control of a quarter car nonlinear active suspension system. *2007 Asia-Pacific Conference on Applied Electromagnetics Proceedings, APACE2007*.
- Gysen, B. L. J., Paulides, J. J. H., Janssen, J. L. G., and Lomonova, E. A. (2010). Active electromagnetic suspension system for improved vehicle dynamics. *IEEE Transactions on Vehicular Technology*, 59(3), 1156-1163.
- Shim, T., and Velusamy, P. C. (2011). Improvement of vehicle roll stability by varying suspension properties. *Vehicle System Dynamics*, 49(1-2), 129-152.
- Cao, D., Song, X., and Ahmadian, M. (2011). Editors' perspectives: road vehicle suspension design, dynamics, and control. *Vehicle System Dynamics*, 49(1-2), 3-28.
- Zeinali, M., and Darus, I. Z. M. (2012). Fuzzy PID controller simulation for a quarter-car semi-active suspension system using Magnetorheological damper. *2012 IEEE Conference on Control, Systems & Industrial Informatics*, 104-108.
- Alvarez-Sánchez, E., (2013). A quarter-car suspension system: car body mass estimator and sliding mode control. *Procedia Technology*, 7, 208-214.
- Van Der Sande, T. P. J., Gysen, B. L. J., Besselink, I. J. M., Paulides, J. J. H., Lomonova, E. A., and Nijmeijer, H. (2013). Robust control of an electromagnetic active suspension system: Simulations and measurements. *Mechatronics*, 23(2), 204-212.
- Turnip, A., and Panggabean, J. H. (2020). Hybrid controller design based magneto-rheological damper lookup table for quarter car suspension. *Int. J. Artif. Intell*, 18(1), 193-206.
- Wang, R., Sheng, F., Ding, R., Meng, X., and Sun, Z. (2021). Vehicle attitude compensation control of magneto-rheological

- semi-active suspension based on state observer. Proceedings of the Institution of Mechanical Engineers, Part D: Journal of Automobile Engineering, 235(14), 3299-3313.
12. Kumar, J., and Bhushan, G. (2022). Dynamic analysis of quarter car model with semi-active suspension based on combination of magneto-rheological materials. *International Journal of Dynamics and Control*, 1-9.
 13. Jamadar, M. E. H., Desai, R. M., Saini, R. S. T., Kumar, H., and Joladarashi, S. (2021). Dynamic analysis of a quarter car model with semi-active seat suspension using a novel model for magneto-rheological (MR) damper. *Journal of Vibration Engineering & Technologies*, 9(1), 161-176.
 14. Pang, H., Wang, Y., Zhang, X., and Xu, Z. (2019). Robust state-feedback control design for active suspension system with time-varying input delay and wheelbase preview information. *Journal of the Franklin Institute*, 356(4), 1899-1923.
 15. Meng, Q., Qian, C., and Liu, R. (2018). Dual rate sampled data stabilization for active suspension system of electric vehicle. *International Journal of Robust and Nonlinear Control*, 28(5), 1610-1623.
 16. Min, X., Li, Y., and Tong, S. (2020). Adaptive fuzzy output feedback inverse optimal control for vehicle active suspension systems. *Neurocomputing*, 403, 257-267.
 17. Pusadkar, U. S., Chaudhari, S. D., Shendge, P. D., and Phadke, S. B. (2019). Linear disturbance observer based sliding mode control for active suspension systems with non-ideal actuator. *Journal of Sound and Vibration*, 442, 428-444.
 18. Chen, L., Xu, X., Liang, C., Jiang, X. W., and Wang, F. (2022). Semi-active control of a new quasi-zero stiffness air suspension for commercial vehicles based on H_2/H_∞ state feedback. *Journal of Vibration and Control*, 10775463211073193.
 19. Viadero-Monasterio, F., Boada, B. L., Boada, M. J. L., and Díaz, V. (2022). H_∞ dynamic output feedback control for a networked control active suspension system under actuator faults. *Mechanical Systems and Signal Processing*, 162, 108050.
 20. Thompson, A. (1976). An active suspension with optimal linear state feedback. *Vehicle System Dynamics*, 5 (4), 187-203.
 21. Thompson, A. and Davis, B. (1989). Optimal linear active suspensions with vibration absorbers and integral output feedback control. *Vehicle System Dynamics*, 18(6), 321-344.
 22. Cheok, K.C., Loh, N.-K., McGee, H.D. and Petit, T.F. (1985). Optimal model-following suspension with microcomputerized damping. *Industrial Electronics, IEEE Transactions on*, No. 4, 364-371.
 23. Esmailzadeh, E. and Taghirad, H. (1998). Active vehicle suspensions with optimal state-feedback control. *International Journal of Modelling and Simulation*, 18, 228-238.
 24. Aubouet, S., Dugard, L. and Sename, O. (2009). H_∞/lpv observer for an industrial semi-active suspension. *Control Applications, (CCA) & Intelligent Control*, 756-763.
 25. Lin, J.-S. and Kanellakopoulos, I. (1997). Nonlinear design of active suspensions. *Control Systems, IEEE*, 17(3), 45-59.
 26. Sam, Y.M., Osman, J.H. and Ghani, M.R.A. (2004). A class of proportional-integral sliding mode control with application to active suspension system. *Systems & Control Letters*, 51(3), 217-223.
 27. Foda, S. G. (2000). Fuzzy control of a quarter-car suspension system. Proceedings of the International Conference on Microelectronics, ICM, 231-234
 28. Yoshimura, T. (1996). Active suspension of vehicle systems using fuzzy logic. *International Journal of Systems Science*, 27(2), 215-219.
 29. Rao, M. and Prahlad, V. (1997). A tunable fuzzy logic controller for vehicle-active suspension systems. *Fuzzy Sets And Systems*, 85(1), 11-21.
 30. Campos, J., Lewis, F., Davis, L. and Ikenaga, S. (2000). Backstepping based fuzzy logic control of active vehicle suspension systems. in *American Control Conference, Proceedings of IEEE*, 6, 4030-4035.
 31. Lauwerys, C., Swevers, J. and Sas, P. (2005). Robust linear control of an active suspension on a quarter car test-rig. *Control Engineering Practice*, 13(5), 577-586.
 32. Park, S. and Rahmdel, S. (2013). A new fuzzy sliding mode controller with auto-adjustable saturation boundary layers implemented on vehicle suspension. *International Journal of Engineering-Transactions C: Aspects*, 26(12), 1401.
 33. Mustafa, G. I., Wang, H., and Tian, Y. (2019). Model-free adaptive fuzzy logic control for a half-car active suspension system. *Studies in Informatics and Control*, 28(1), 13-24.
 34. Nagarkar, M., Bhalerao, Y., Bhaskar, D., Thakur, A., Hase, V., and Zaware, R. (2022). Design of passive suspension system to mimic fuzzy logic control active suspension system. *Beni-Suef University Journal of Basic and Applied Sciences*, 11(1), 1-15.
 35. Khodadadi, H., and Ghadiri, H. (2018). Self-tuning PID controller design using fuzzy logic for half car active suspension system. *International Journal of Dynamics and Control*, 6(1), 224-232.
 36. Bingül, Ö., and Yıldız, A. (2022). Fuzzy logic and proportional integral derivative based multi-objective optimization of active suspension system of a 4×4 in-wheel motor driven electrical vehicle. *Journal of Vibration and Control*, 10775463211062691.
 37. Yatak, M. Ö., and Şahin, F. (2021). Ride comfort-road holding trade-off improvement of full vehicle active suspension system by interval type-2 fuzzy control. *Engineering Science and Technology, an International Journal*, 24(1), 259-270.
 38. Özdemir, A. ve Maden D. (2013). Aktif süspansiyon sistemli çeyrek araç modelinin gözlemleyiciyle optimal kontrolü. *SAÜ. Fen Bil. Der.*, 17(2), 181-187.
 39. Palm, W., J., (2010). *System Dynamics Second Edition*, McGraw-Hill, Newyork, Usa, 807.
 40. Al-Ghanim, A. M. H. and Nassar, A. A. (2018). Modeling, simulation, and control of half car suspension system using Matlab/Simulink. *International Journal of Science and Research (IJSR)*, 7(1), 351-362.
 41. Palanisamy, S. and Karuppan, S. (2016). Fuzzy control of active suspension system. *JVE International LTD. Journal of Vibroengineering*, 18(5), 3197-3204.
 42. Salem, M. M. M. and Aly, A. A. (2009). Fuzzy control of a quarter-car suspension system. *International Journal of Computer and Information Engineering*, 3(5), 1277-1281.



Autonomous Feed Pushing Robot Design and Manufacturing

Ahmet Uyumaz^{1*}, Şenol Güzel², Abdullah Köse¹, Sinan Satılmış¹, Burak Polat¹
Oğuzhan Karakaş¹, Yiğitcan Küçükçelen¹

¹Mechanical Engineering Department, Faculty of Engineering and Architecture, Burdur Mehmet Akif Ersoy University, Burdur, 15030, Turkey

²Department of Molecular Biology and Genetics, Faculty of Science and Literature, Burdur Mehmet Akif Ersoy University, Burdur, 15030, Turkey

ABSTRACT

The inability of animals to reach the food during feeding causes stress and may lead to a decrease in milk yield. At this point, adequate nutrition of animals in farms is very important in terms of milk yield. In this study, the design and manufacture of an autonomous machine that can be used in animal farms and facilities has been carried out. The functions of the device were determined and the main chassis and the parts were designed. First, the main chassis, which forms the body of the device was designed and electronic components were assembled on it. Feed is pushed by means of the drum, which is mounted on the main chassis with the connecting arms and located outside. The device was produced with the designed machine body. The machine can provide forward-backward, rotational and drum movements. It has a mass of approximately 80 kg and is equipped with three 12 V direct current electric motors. The device, which can be operated with Arduino and interface program, can move autonomously. The machine designed and manufactured has been tested in the animal farm.

Keywords: Autonomous, Feed pushing robot, Milk yield, Labor

History

Received: 14.09.2022

Accepted: 07.11.2022

Author Contacts

<http://dx.doi.org/10.29228/eng.pers.66804>

*Corresponding Author

e-mail addresses : auyumaz@mehmetakif.edu.tr*, sguzel@mehmetakif.edu.tr, kose.abdullah@icloud.com, satilmisinann@gmail.com, buraakpoolat@gmail.com, karakask_oguzhan@hotmail.com, yigitcankucuk-celen@gmail.com

Orcid numbers : 0000-0003-3519-0935, 0000-0002-5811-7979, 0000-0001-8826-2272, 0000-0002-2855-9338, 0000-0003-0549-3177, 0000-0002-8076-147X, 0000-0003-1894-5515

1. Introduction

Autonomous era is rapidly spreading with developing technology in the world. The tools and equipment that we use frequently show that the autonomous age has developed. With the rapid developing of the industry 4.0 era and the Industry 5.0 era, the autonomous is frequently encountered every day [1-4]. Most of the devices we see around us are actually examples of the rapid development of the autonomous era. Autonomous technologies are widely used in the automotive industry, aviation, textile, agriculture and livestock fields [5-9].

One of the biggest benefits of autonomous technology is eliminating man power. It is used as a useful purpose by eliminating man power in many areas and increasing the technological development and welfare levels of countries thanks to artificial intelligence. There are serious developments in many areas, from driverless cars to space technology and defense industry in autonomous technology. Protecting human health and causing less harm to the environment and atmosphere are some of the most important advantages of this

technology. With this developing technology, time, energy and labor can be saved in the area where it is used [1-9]. Due to the increase and development of animal husbandry in the developing agricultural sector of our country in recent years, animal breeding in farms is increasing day by day. The nutritional needs and other needs of animals are met with the contribution of man power. At this point, the human factor in the agricultural sector comes first and the need for man power increases. However, this brings additional labor costs. As mentioned before, the cost of equipment used in farms and animal facilities is quite high, and the employment of labor brings extra costs. So, owners and farmers cannot afford this costs. Because, manpower is always needed to push the feed in front of the animals resulting in extra expense for the farm. Therefore, the usage of autonomous technologies in the field of agriculture comes to the fore [4-9].

Import and export of milk and dairy products in our country are one of the most important parameters in the agriculture and livestock

sector. The total number of animals milked in our country is approximately 33 million in 2020, and milk export is around 517 million dollars [10-12]. Animal breeding, animal care and the amount of milk obtained from animals are important issues that we encounter in the field of agriculture in the world. In order to increase the milk obtained from animals, it is necessary to meet the nutritional needs and care of animals in the most efficient and healthy way according to environmental conditions. Keeping the environment clean and spacious, timely and appropriate feeding and usage of some vehicles such as tractors or any other machines according to time and conditions are very important for the milk yield and health. Feeding animals with the help of tractors not only emit harmful exhaust gases but also produces high level of noise due to internal combustion engines. On the other hand, necessity of fuel is required in case of usage of internal combustion engines. The released harmful gases affect adversely the health of both farm workers and animals. At the same time, equipment used with man power can cause animals to be afraid. One of the most significant problem is poor nutrition, because animal moves the feed away from its front. Worry about not being able to keep up with the food can also cause stress in animals. As a result, it is seen that milk yield decreases in malnourished animals. In the mean time, it has been observed that the number of heart beats is higher during eating than standing [13-16]. It is even known that milk yield is affected by stress experienced by animals during feeding [13-18]. Residual feed is another problem in animal farms. Residual feed can be also eliminated with devices that automatically push feed in front of animals without the need for manpower. Activities and development studies that will increase productivity in the animal husbandry sector are of great importance in our country, where there are approximately 18 million cattle [19,20]. At this point, milk yield, which provides great benefit in cattle breeding, is one of the most important arguments for our country in this field. It is seen that the share of cattle in milk production has exceeded 90% as of 2017 [10-12].

When time schedule of cattle was examined, it was determined as 42.4% resting, 11.1% standing, 32.3% feeding, 1.6% drinking water, 6.3% walking, 1.7% other behaviors and 4.6% milking. As it is seen that feeding is a big part of it. At this point, animals were observed with cameras for 24 hours. It has been found that high productivity was determined on animals, which were kept away from stress [21]. It was also presented that the factors that cause stress in animals should be carefully examined and practices aimed at eliminating these factors should be implemented. It is seen that deterioration of hygiene in the environment where the animal lives, decrease the amount and quality of feed and the loss of weight of animals are natural responses to stress [17,22]. At the same time, stress negatively affects the lactation period. It negatively affects milk production by causing a decrease in oxytocin hormone production during stress [18, 23-29].

As stated earlier, labor cost is rather high for farmers. It was showed that the largest expense ratio after feed costs is temporary workers in the farm. It is seen that this value is 1.98% of the enterprise average [30]. It is seen that these costs can be reduced with the usage of some autonomous devices.

The usage areas in farms change according to the parameters of produced autonomous robots and their types. Autonomous robots can run according to nutritional needs of animals in the farm. They

perform the tasks that they have to do in specified time intervals. They also take on the tasks instead of human with the help of their software resulting in reducing environmental pollution. Animal husbandry can be done efficiently with robots that are operated according to farm conditions without harming the environment and animals.

There are autonomous devices that have been used to push the feed in front of animals or devices that perform different tasks in agriculture and livestock industry. They have mobile applications and have battery-powered systems [7,31-35]. However, these products are quite expensive to buy. In this study, the design and manufacture of an autonomous feed pushing robot working with a direct current battery was carried out. It was aimed to design and manufacture an economical and efficient feed pushing robot. Feed can be moved away from animals while feeding. The autonomous feed pushing robot will be able to push feed in front of the animals with the help of rotating plate and rubber. The produced machine can be used in covered farms with concrete floors. After completing its mission, the autonomous robot can come to the charging station to recover its energy and prepare for the next tour. The manufactured robot is autonomous and can eliminate the need for labor. It was also aimed that produced autonomous robot will be a device that users and farmers can easily buy and use economically. This will result in substantial financial gain.

2. Material and Method

In this study, autonomous feed pushing robot was designed using Solidworks. Designed mechanical chassis and sheet drum are seen in Figure 1. Manufactured device can be divided into two sections called mechanical and automation system. Mechanical section consists of main frame, shaft, wheels, brackets, iron blade and profile, chain gear mechanisms, sheet drum and top cover. On the other hand, there are three DC electric motor, 12V DC battery, rotary encoder, relay, potentiometer, sensor, limit switches, Arduino microcontroller, safety button and control panel in the automation system.



Figure 1. General view of the chassis and designed autonomous robot for the feed pushing

Main frame of the device and some components are seen in Figure 2. Designed device can move forward, backward, right, left, and the drum can be rotated using DC electrical motors. The movement of the mechanism is provided via front wheel powered by electric motor. Driving electric motors were powered by 12V DC battery in automation system. The automation system generally consists of sensors, safety system, power supply and control panel parts as seen in Figure 3. Relays which are economical and practical method were utilized to drive DC motors. Microcontroller has been used in order to control relays. In addition, progress of the distance and position of the steering should be determined. Potentiometer and rotary encoder

were used to do these tasks. Dead reckoning method has been applied using distance, time and direction information. The signals produced by the rotary encoder and potentiometer can be received by the microcontroller and the electric motors can be driven.

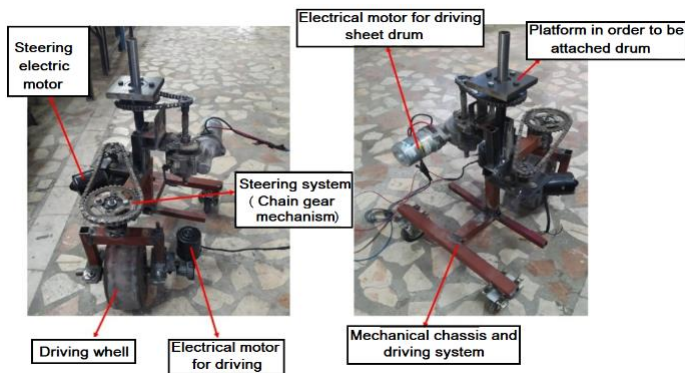


Figure 2. Mechanical main frame of the device and some components

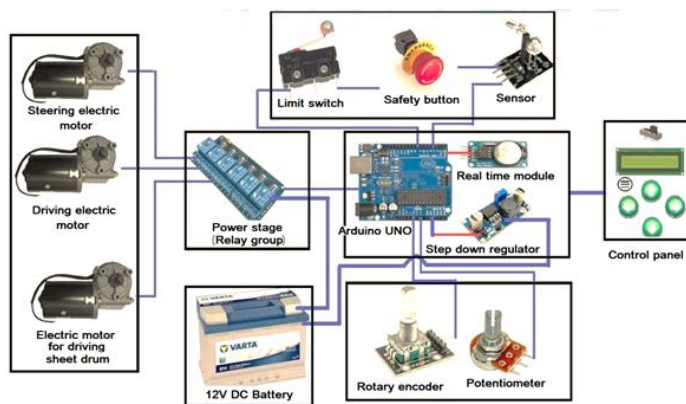


Figure 3. Automation system and components

The automation system of the autonomous feed pushing robot has manual and operator modes and the robot can be operated in both modes. It can be controlled by a wired controller in manual mode. In manual mode, the route to be followed in the facility is firstly shown to the robot. With this tour, data from the rotary encoder and steering position sensor can be recorded by the robot during route determination. Registration ends at the last charging station. If the autonomous robot is in operator mode, automation algorithm starts at the lap times entered into the microcontroller. The encoder and steering position data previously saved in the memory can be compared with the new data and the motors can be driven. The route within the facility starts at the charging station and ends at the charging station. After the autonomous robot completes the designated tour, it can come to the charging station where the batteries can be charged. User can be able to program the robot without the need for a technical personnel. Block circuit diagram for driving motors is presented in Figure 4. In addition, an algorithm has been created for the control and automation of the robot. The automation algorithm of the autonomous robot is shown in Figure 5.

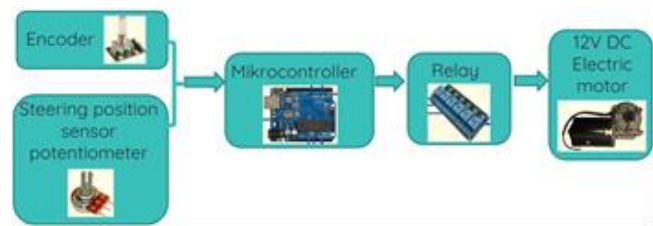


Figure 4. Block circuit diagram for driving motors

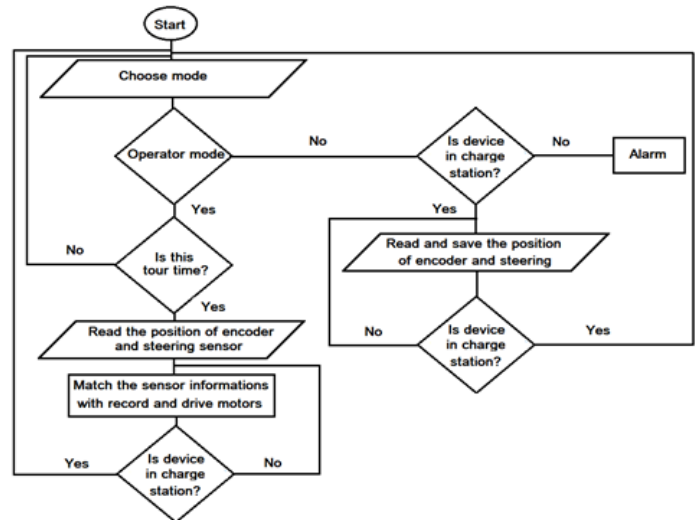


Figure 5. Autonomous feed pushing robot automation algorithm

3. Results and Discussion

Nutrition of animals is critical for milk yield and animal health. It is essential to have sufficient feed in front of the animals, especially in farms and facilities where there are many animals. There is now a need for a labor force to reduce feed and adequate nutrition. However, labor force requires extra costs for this task in the animal farms. Besides, extra time is spent for pushing feed to the front of the animals. Figure 6 shows the schematic representation of the feed pushing.

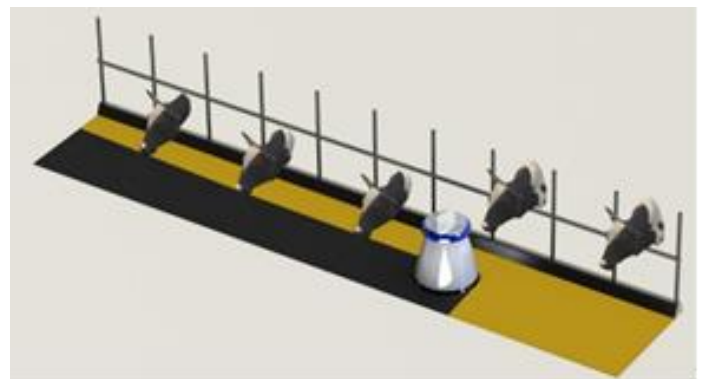
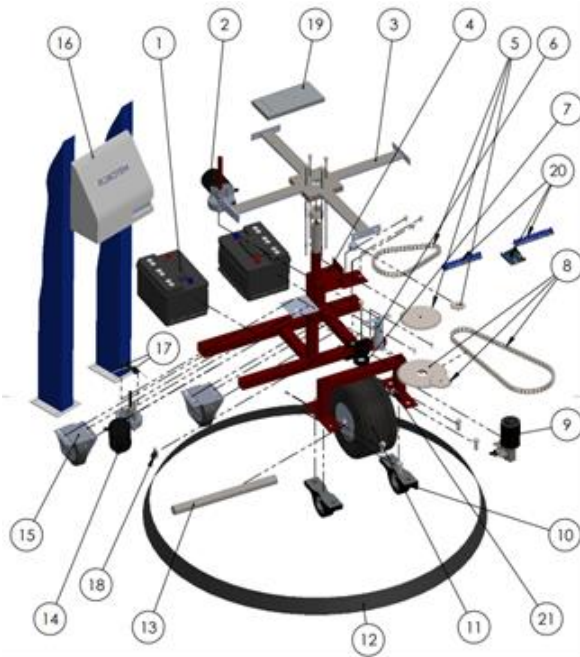


Figure 6. Schematic representation of the feed pushing

The agriculture and livestock sector in our country is developing day by day with technology. With the developing technology of our country, it is very important that the development in every field is through the production of domestic and national products. It was also

aimed to design original machine and produce in this study for pushing feed. Rail systems can be used to push feed in animal farms. However, maintenance costs are high. On the other hand, when machines with internal combustion engines that perform this process are used, there is fuel consumption and harmful gases are released. At the same time, manpower is needed to push the feed. Since the system is electric and autonomous, these problems are eliminated in the current study. The design of the machine has been created taking into account the strength and the characteristics of the work to be done. Attention was paid to the weight, balance and ability to carry the parts on the device. It is important that there are no mechanical problems such as wear and friction during the usage of robot. Figure 7 exhibited the explosion view of the autonomous feed pusher robot.



1. Battery 2. Steering electric motor 3. Drum connection cross 4. Connection bracket 5. Steering gears and chain 6. Front wheel hitch pin 7. Front wheel hitches 8. Drum drive gears and chain 9. Forward-reverse electric motor 10. Front axle joint 11. Drive wheel 12. Rubber hoop 13. Front axle 14. Drum electric motor 15. Rear wheel 16. Charging station 17. Switches limiting left and right movement 18. Steering position sensor 19. Remote control 20. Autonomous control system 21. Encoder

Figure 7. Explosion view of the autonomous feed pusher robot

The most important side of this study is to design and manufacture device that uses less energy. For this purpose, electric energy is utilized for pushing feed. In this case, the determination of the operation current is critical. So, each electric motor uses about 3 amper current. If 72 Ah DC battery is used, all electric motors can be run at about 8 hours with full charge. So the determination of required power is essential for electric motors. On an average-sized farm, animals are fed about 5 or 6 times a day. One period can be completed via the stored energy thanks to the used 12V DC battery. When each feeding takes about 15 minutes for an average sized farm, machine can easily do many tours. As it is known, required power can be calculated according the weight and motions of the machine as mentioned below.

$$P = T \cdot \omega \quad (W) \quad (1)$$

$$\omega = \frac{2\pi n}{60} \quad (rad / sn) \quad (2)$$

$$P = F \cdot V \quad (W) \quad (3)$$

Where P, T and ω refers to power, engine torque and angular velocity. F and V defines the force and velocity [36,37]. Figure 8 shows the manufactured feed pushing robot.



Figure 8. Manufactured feed pushing robot

4. Conclusions

Autonomous feed pushing robot provides a more efficient and more comfortable opportunity by eliminating human power and eliminating the damages and losses that may occur. It saves both time and efficiency, and offers a more comfortable technology that can adjust itself to environmental farm conditions. In this study, it was aimed to design and produce autonomous feed pushing robot. Manufactured device was tested in an animal farm. Each feeding process can take about 15 minutes on an average sized farm. If 5 periods are taken into account 450 hours of labor per year can be saved. If a farm that produces 100 liters of milk per day is considered, increase in production milk 3-5 liters per day and a total 1100-1800 liters in a year will be estimated. Total cost of the autonomous feed pushing robot is about \$600 which is very less compared to the other brands. Malnutrition can be prevented with designed device and the efficient usage of manpower will be ensured. The amount of residual feed decreases in front of the animals. In addition, labor costs can be reduced for pushing feed. Since manufactured device is not so expensive, it can be used in small and medium-sized farms apart from in large farms. According to the findings of this study, the robots used by the farmers around the world in their farms are rapidly becoming widespread each passing day.

Acknowledgment

We would like to thank the Turkish Technology Team Foundation and the Ministry of Industry and Technology for their support in the design and manufacturing of the Autonomous Feed Pushing Robot for organizing the Teknofest Aviation, Space and Technology Festival. We also thank to Burdur Mehmet Akif Ersoy University, UMT Molding Firm and Hüseyin Kütük for their support and Prof. Dr.

Şenol Güzel who is director of Burdur Mehmet Akif Ersoy University Agriculture, Livestock and Food Applications Research Center, in order to give us chance and allow usage and test of the produced machine in Burdur Mehmet Akif Ersoy University Animal Farm.

Nomenclature

F	Force (N)
DC	Direct current
P	Power output (W)
T	Torque (Nm)
V	Velocity (m/s)
ω	Angular velocity (rad/s)
n	Engine speed (rpm)

Conflict of Interest Statement

The authors declare that there is no conflict of interest in the study.

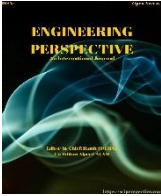
CRedit Author Statement

Ahmet Uyumaz: Conceptualization, Supervision, Project administration, Writing-original draft, Validation, Writing-review&editing
Şenol Güzel: Conceptualization, Supervision, Project administration
Abdullah Köse: Validation, Project administration, Data curation, Methodology Formal analysis
Sinan Satılmış: Methodology, Funding acquisition, Validation, Software
Burak Polat: Funding acquisition, Investigation, Resources
Oğuzhan Karakaş: Methodology, Investigation, Resources
Yiğitcan Küçükçelen: Data curation, Investigation, Methodology

References

- Ertuğrul, İ., Deniz, G., (2018). 4.0 Dünyası: Pazarlama 4.0 ve Endüstri 4.0. Journal of Bitlis Eren University Institute of Social Sciences, 7(1): 158-170.
- Sadıç, Ş., (2022). Endüstri 5.0 ve Sürdürülebilirlik. In book: Endüstri 5.0 Dijital Toplum Publisher: Preprint, Türkiye.
- Terzi, A., (2021). Endüstri 4.0 Sürecinde Üretim Maliyetlerinde Meydana Gelmesi Beklenen Etkiler Üzerine Bir İnceleme. Muhasebe ve Vergi Uygulamaları Dergisi, 14 (2): 837-872.
- Toplum 5.0. (2022). Bilgi Teknolojileri ve İletişim Kurumu. <https://www.btk.gov.tr/uploads/pages/arastirma-raporlari/toplum-5-0-arastirma-raporu.pdf> (Date of Access: 25.11.2022).
- Çevik, M., (2021). Tarımda Teknoloji Verimlilik ve Tasarruf Sağlıyor. Tarım ve Orman Dergisi, <http://www.turktarim.gov.tr/Haber/619/tarimda-teknoloji-verimlilik-ve-tasarruf-sagliyor> (Date of Access: 25.11.2022).
- Fukuyama, M., (2018). Society 5.0: Aiming for a New Human-Centered Society. Japan Spotlight, https://www.jef.or.jp/journal/pdf/220th_Special_Article_02.pdf
- Güzey, A., Akıncı, M.M., Altan, Ş., (2020). Otonom Kara ve Hava Araçları ile Akıllı Tarım: Hasat Optimizasyonu Üzerine Bir Uygulama. Ankara Hacı Bayram Veli Üniversitesi İktisadi ve İdari Bilimler Fakültesi Dergisi, Özel Sayı:207-220.
- Saracel, N., Aksoy, I., (2020). Toplum 5.0: Süper Akıllı Toplum. Social Sciences Research Journal, 9 (2): 26-34.
- Akıllı Tarım (2022). Akıllı Tarım. Bilgi Teknolojileri ve İletişim Kurumu. <https://www.btk.gov.tr/uploads/pages/arastirma-raporlari/akilli-tarim.pdf> (Date of Access: 25.11.2022).
- Ataseven, Z.Y., (2020). Tarımsal Ekonomi ve Politika Geliştirme Enstitüsü, Durum ve Tahmin Süt ve Süt Ürünleri. <https://arastirma.tarimorman.gov.tr/tepge/Belgeler/Yay%C4%B1n%20Ar%C5%9Fivi/2017-2022%20Yay%C4%B1n%20Ar%C5%9Fivi/Yay%C4%B1nno321.pdf> (Date of Access: 25.11.2022).
- Ataseven, Z.Y., (2021). Tarımsal Ekonomi Ve Politika Geliştirme Enstitüsü, Durum ve Tahmin Süt ve Süt Ürünleri. <https://arastirma.tarimorman.gov.tr/tepge/Belgeler/PDF%20Durum-Tahmin%20Raporlar%C4%B1/2021%20Durum-Tahmin%20Raporlar%C4%B1/S%20C3%BCt%20ve%20S%20C3%BCt%20C3%9Cr%20C3%BCnleri%20Durum%20Tahmin%20Raporu%202021-331%20TEPGE.pdf>, (Date of Access: 25.11.2022).
- TÜİK, (2019). Hayvancılık İstatistikleri, Süt ve Süt Ürünleri Verileri. <https://data.tuik.gov.tr/Bulten/Index?p=Hayvansal-Uretim-Istatistikleri-2019-33873>, Date of Access: 25.11.2022).
- Cengiz, F., (2001). Hayvanlarda Zorlanım (Stres) Oluşturan Etkenler. Uludağ Üniversitesi Veteriner Fakültesi Dergisi, 20, 147-153.
- Hall, S.J.G.; Forsling, M.L.; Broom, D.M., (1998). Stress responses of sheep to routine procedures changes in plasma concentrations of vasopressin, oxytocin and cortisol. Veterinary Record. 142 (4) 91-93.
- Hall, S.J. G.; Broom, D.M.; Goode, J.A.; Lloyd, D.M.; Parrott, R.F.; Rodway, R.G., (1999). Physiological responses of sheep during long road journeys involving ferry crossings. Animal Science. 69:19-27.
- Parrott, R.F.; Hall, S.J.G.; Lloyd, D.M., (1998). Heart rate and stress hormone responses of sheep to road transport following two different loading procedures. Animal Welfare. 7(3) 257-267.
- Altınçekiç, Ş., Ö., Koyuncu, M., (2012). Çiftlik Hayvanları ve Stres, Hayvansal Üretim 53(1): 27-37
- Pehlivan, E., Dellal, G., (2014). Memeli Çiftlik Hayvanlarında Stres, Fizyoloji ve Üretim İlişkileri. Hayvansal Üretim 55(1): 25-34.
- TÜİK, (2021). Hayvansal Üretim İstatistikleri, <https://data.tuik.gov.tr/Bulten/Index?p=Hayvansal-Uretim-Istatistikleri-Haziran-2021-37208#:~:text=T%C3%9C%C4%B0K%20Kurumsal&text=B%C3%BCy%C3%BCkba%C5%9F%20hayvanlar%20aras%C4%B1nda%20yer%20alan,194%20bin%20ba%C5%9F%20olarak%20ger%C3%A7ekle%C5%9Fti>. (Date of Access: 25.11.2022).
- Ulusal Süt Konseyi, (2022). Ulusal Süt Konseyi, Süt ve Süt Ürünleri Dış Ticareti, <https://ulusalsutkonseyi.org.tr/disticaret/> (Date of Access: 25.11.2022).
- Uzal, S., (2008). Serbest ve Serbest Duraklı Süt Sığırcı Barınaklarında Hayvanların Alan Kullanımı ve Zaman Bütçesine Mevsimlerin Etkisi, Doktora Tezi, Selçuk Üniversitesi Fen Bilimleri Enstitüsü, Konya.
- Martin, S.W., Schwabe, C.W., Franti, C.E. (1975). Dairy calf mortality rate: Influence of meteorological factors on calf mortality rate in Tulare County, California. Am. J. Vet. Res. 36: 1105-1109.
- Bruckmaier, R.M. (2005). Normal and disturbed milk ejection in dairy cows. Domest. Anim. Endocrinol. 29: 268-273.
- Bobic, T., Mijic, P., Knezevic, M., Speranda, B., Antunovic, B., Baban, M., Sakac, M., Frizon, E., Koturic, T. (2011). The impact of environmental factors on the milk ejections and stress of dairy cows. Biotech. Anim. Husb. 27(3): 919-927.
- Dahl, G.E. (2008). The eighth international workshop on the biology of lactation in farm animals: Introduction. J. Anim. Sci. 86(Suppl. 1): 1-2.

26. Matteri, R. L., Carroll, J. A., Dyer, C. J. (2000). Neuroendocrine responses to stress. Ed. Moberg G.P., Mench, J.A. The Biology of Animal Stress: Basic Principles and Implications for Animal Welfare. CABI Publishing, USA.
27. Munsterhjelm, C. (2009). Housing, stress and productivity: studies in growing and reproducing pigs. University of Helsinki, Academic Dissertation, Helsinki.
28. Squires, E. J. (2003). Applied animal endocrinology. CABI Publishing, USA.
29. Yadav, S., Anand, M. (2013). Stress and lactation: an overview. Ed. Yadav, S., Kumar, J., Madan, A.K., Yadav, B., Anand, M. Physiology and Nutri-Genomics, Underpinning Animal Production. India.
30. Byashimov, G., (2012). Hayvancılık İşletmelerinin Ekonomik Analizi ve Rekabet Stratejisi; Türkmenistan Marı İli Yolöten İlçesi Örneği, Yüksek Lisans Tezi, Selçuk Üniversitesi Fen Bilimleri Enstitüsü, Konya.
31. Dikbaş, S., (2021). ZT Traktör - Otonom Tarım Traktörü. <https://www.tarimsalteknoloji.com/zt-traktor-otonom-tarim-traktoru-123#>, (Date of Access: 25.11.2022).
32. Delaval (2018). Yeni DeLaval OptiDuo Sadece Yem İtmiyor. <https://www.mutluciftlikler.com/post/yeni-delaval-optiduo-sadece-yem-i-CC%87tmiyor>, (Date of Access: 25.11.2022).
33. Fermanet (2022). Yemleme Robotu Cow-boy. <https://fermanet.com/urun/yemleme-robotu/> (Date of Access: 25.11.2022).
34. Lely Juno, (2022). Otomatik Yem İtici. <https://www.lely.com/tr/cozumler/yemleme/juno/> (Erişim Tarihi: 25.11.2022)
35. Metfarm, (2016). Yem İtme Robotu-FRONE. <https://www.metfarm.com/yem-itme-robotu-frone/> (Date of Access: 25.11.2022).
36. Çengel, Y.A., Jimbala, J.M., (2008). Akışkanlar Mekaniği Temelleri ve Uygulamaları. Güven Bilimsel, İzmir Güven Kitabevi. İzmir, Türkiye.
37. Çetinkaya, S., (2017). Taşıt Mekaniği. Nobel Akademik Yayıncılık Eğitim Danışmanlık Tic. Ltd. Şti. Ankara, Türkiye.



Investigation of Natural Frequency Values of Composite Cover Design with Different Laying Angles

Mehmet Can Katmer^{1,2}, Adnan Akkurt², Tolga Kocakulak^{3*}

¹Hidromek A.Ş., Sincan Organized Industrial Zone, Ankara, TURKEY

²Gazi University, Faculty of Technology, Department of Industrial Design Engineering, Ankara, TURKEY

³Burdur Mehmet Akif Ersoy University, Technical Sciences of High Vocational School, Burdur, TURKEY

ABSTRACT

In this study, the effect of composite laying angle on the natural frequency values of a long and flexible cover made of laminated composite material was investigated. Investigation of the effect of the laying angle, a composite cover with rib design with the topography optimization method was used. The cover design used in the study is an industrial design product and has producible features. A design with a total of 20 different laying angles has been made on the ribbed and ribless parts of the composite cover. Care was taken that the selected laying angles do not interfere with manufacturability. Designs with different laying angles are modeled with the ANSYS ACP module. The modal analysis of the created designs was carried out with the finite difference method in the ANSYS program environment. As a result of the modal analysis, natural frequency values of mode 1, mode 2, mode 3, mode 4, mode 5 and mode 6 of these designs were obtained. It was concluded that the best mode 2 natural frequency values (45°, -45°, 45°, -45°, 45°, -45°, 45°) were obtained by using the degree of laying angles. In this design, mode 2 has a natural frequency value of 12.2 Hz, mode 3 33 Hz, mode 4 40.9 Hz, mode 5 57.8 Hz and mode 6 82.7 Hz. In this design, mode 2 has a natural frequency value of 12.2 Hz, mode 3 33 Hz, mode 4 40.9 Hz, mode 5 57.8 Hz and mode 6 82.7 Hz.

Keywords: Laying angle, Composite, Natural frequency, Design, Modal analysis

History

Received: 04.10.2022

Accepted: 03.12.2022

Author Contacts

*Corresponding Author

e-mail addresses : mehmet.katmer@hidromek.com.tr, aakkurt@gazi.edu.tr,

tkocakulak@mehmetakif.edu.tr*

Orcid numbers : 0000-0002-4610-8178, 0000-0002-0622-1352, 0000-0002-1269-6370

<http://dx.doi.org/10.29228/eng.pers.66826>

1. Introduction

Composite materials are widely used in sectors such as the automotive industry, aerospace and defense industry due to various advantages [1,2]. Composite is defined as a material with different new properties by combining two or more materials [3,4]. With the use of composite materials increasing day by day, the studies have gained intensity. The most basic common goal in these studies can be said to reduce design weight and achieve better mechanical performance [5,6,7]. One of the most basic methods of achieving this goal is the use of layered type composite structures [8,9]. Although it has these features, studies are continuing to improve it and eliminate some of the problems it carries [9]. The most important of these problems aimed to be solved is the vibration behavior of composite materials [10].

structure around its equilibrium position. In many systems used in engineering and daily life, vibrations occur due to environmental or undetected reasons. Long-term vibration can cause fatigue in the machine elements and cause breakage and damage. In particular, the determination of vibrations and values of structures used in critical functions are important for natural frequency values and resonance issues. The modal analysis method is widely used to predict the vibration properties of a designed structure. The purpose of the modal analysis is to determine the natural frequencies and the corresponding mode behaviors [11,12,13,14].

Studies aiming to improve the characteristic properties of layered type composite materials are available in the literature. Şakar et al. observed the effect of orientation angles and a number of layers on the dynamic behavior of the composite structure in the sandwich panels they prepared. The mode shapes and natural frequencies of

Vibratory motion can be defined as the repeated motion of a

the produced panels were determined both experimentally and numerically with the ANSYS program [15]. Athihan studied computational and experimental modal analysis on delaminated composite structures with different orientation angles consisting of 16 paves. He observed the dynamic behavior of the structures according to the orientation angle change and delamination status. He used ANSYS software for analysis studies [16]. R. Gibson explained the modal analysis methods used to determine the dynamic behavior of fiber-reinforced composite materials, the determined parameters and basically what factors will change these parameters [17]. Yeşilyurt et al. in their study, applied modal analysis to a bar produced as a unidirectional composite and approached to determine the mechanical properties of the material with the data obtained [18]. Soni et al. made the most appropriate design study by changing the orientation angles for low displacement and high strength in laminated composite plates. The layer placements were examined as an angled layer, unsymmetrical and symmetrical angled layer [19]. In the second stage of his study, Vatangül numerically investigated the behavior and strength of composite samples with different orientation angles under load. They used ANSYS software in their studies [20]. Baba examined the effects of parameters such as boundary condition, delamination size, location of delamination and fiber orientation angles on plate buckling behavior in composite plates [21]. It has been observed in the literature that many studies have been made and are still being done for the appropriate design of layered composite materials. In these studies, the behavior of the layered composite material; has been observed that fiber orientation angle, layer thickness and number, delamination, temperature, symmetric or non-symmetrical array are examined depending on many different parameters. As a result of the research; In many of the studies on both structural optimization and composite material, it has been determined that the modal analysis method is used to examine the behavior of the part.

In the literature, no study has been found in which the laying angles of the lid, which is an industrial design product and can be produced, and which has a long and flexible design, are examined. In this study, the optimum laying angle design was determined by examining the natural frequency values in case the composite material used in the cover design with a long and flexible structure has different winding angles. Natural frequency values were obtained by the modal analysis method in ANSYS environment.

2. Material and Method

The effect of the laying angles on the natural frequency value of the long and flexible composite cover, of which rib design was made with the topography optimization method, was investigated. The macro mechanics of laminated composite plates are discussed in detail and formulated. Information about the materials and layers of the composite cover is given. 20 different designs were created by applying different laying angles to the ribbed composite cover. A finite element model of designs with different laying angles was created in ANSYS environment. The mesh spacing value was chosen as 5 mm in order not to prolong the processing time more than necessary and to obtain results close to the real values. In addition, analyzes were made at several different mesh spacing values and it was observed that the results differed negligibly at mesh sizes be-

low 5 mm. By applying modal analysis to all designs, natural frequency values of mode 1, mode 2, mode 3, mode 4, mode 5 and mode 6 were obtained.

2.1 Macro Mechanics of Laminated Composite Plates

The representation of a layered composite plate is shown in Figure 1. In Figure 2 and Figure 3, the forces and displacements occurring in the plate are expressed [22].

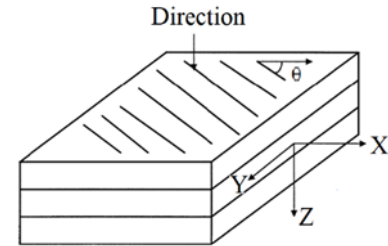


Figure 1. Schematic representation of the laminated composite plate

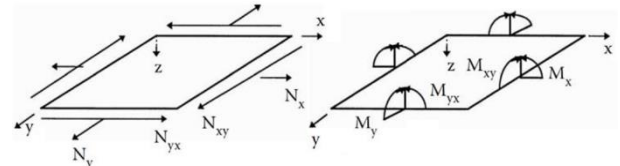


Figure 2. Forces and moments in the laminated composite plate

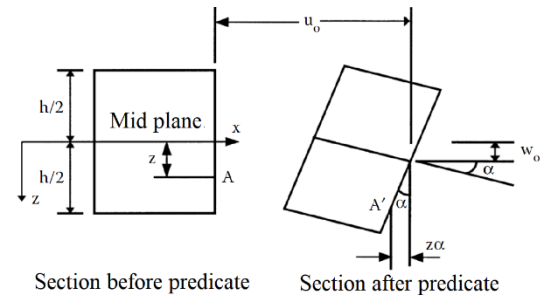


Figure 3. The relationship between displacement and curvature before and after loading

u_0 , v_0 and w_0 show the mid-plane ($z=0$) displacements of the layered composite material in the x, y and z directions. Equations 1, 2 and 3 show the displacements of the u , v and w layered composite material in the x, y and z directions of any point on the cross section.

$$u = u_0 - z\alpha \quad (1)$$

$$\alpha = \frac{\partial w_0}{\partial x} \rightarrow u = u_0 - z \frac{\partial w_0}{\partial x} \quad (2)$$

$$v = v_0 - z \frac{\partial w_0}{\partial y} \quad (3)$$

The unit strain-displacement relations are given in equations 4, 5 and 6.

$$\varepsilon_x = \frac{\partial u}{\partial x} = \frac{\partial u_0}{\partial x} - z \frac{\partial^2 w_0}{\partial x^2} \quad (4)$$

$$\varepsilon_y = \frac{\partial v}{\partial y} = \frac{\partial v_0}{\partial y} - z \frac{\partial^2 w_0}{\partial y^2} \quad (5)$$

$$\gamma_{xy} = \frac{\partial u}{\partial y} + \frac{\partial v}{\partial x} = \frac{\partial u_0}{\partial y} + \frac{\partial v_0}{\partial x} - 2z \frac{\partial^2 w_0}{\partial x \partial y} \quad (6)$$

The unit strains in the midplane and the global strains in terms of curvatures are shown in equation 7.

$$\begin{Bmatrix} \varepsilon_x \\ \varepsilon_y \\ \gamma_{xy} \end{Bmatrix} = \begin{Bmatrix} \frac{\partial u_0}{\partial x} \\ \frac{\partial v_0}{\partial y} \\ \frac{\partial u_0}{\partial y} + \frac{\partial v_0}{\partial x} \end{Bmatrix} + z \begin{Bmatrix} -\frac{\partial^2 w_0}{\partial x^2} \\ -\frac{\partial^2 w_0}{\partial y^2} \\ 2\frac{\partial^2 w_0}{\partial x \partial y} \end{Bmatrix} = \begin{Bmatrix} \varepsilon_{x0} \\ \varepsilon_{y0} \\ \gamma_{xy0} \end{Bmatrix} + \begin{Bmatrix} K_x \\ K_y \\ K_{xy} \end{Bmatrix} \quad (7)$$

Since \bar{Q} varies depending on the mechanical properties and angle of each layer, the stress does not change linearly across the plate, it remains linear only within the layer. In other words, if the elongation and curvature values of the midplane are known, the values of the global stresses (σ_x , σ_y , τ_{xy}) can be found depending on the position (z) as above. Therefore, local stresses and strains can be found for each layer using the transformation matrix and damage criteria can be applied. In Figure 4, the stress and strain variation of the laminated composite plate for the mid-plane, and in Figure 5, the coordinate positions of the layers in the laminated composite plate are given according to the midplane [22].

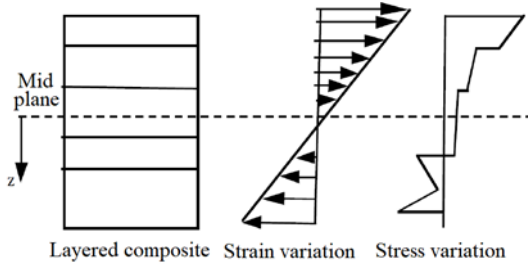


Figure 4. Stress and strain variation along with the thickness of the laminated composite plate

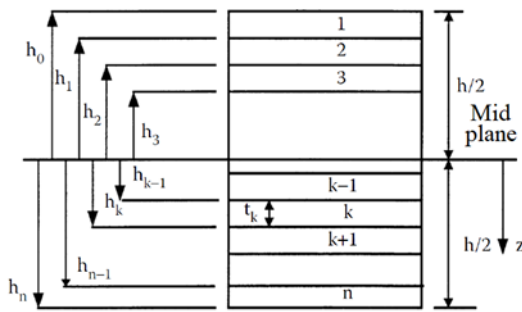


Figure 5. Coordinate positions of the layers in the laminated composite plate

Writing the elongation and curvature values of the midplane in terms of forces and moments is expressed by N_x , N_y and N_{xy} . In-plane normal and shear forces for unit length are shown in equation 8.

$$\begin{Bmatrix} N_x \\ N_y \\ N_{xy} \end{Bmatrix} = \begin{bmatrix} A_{11} & A_{12} & A_{16} \\ A_{12} & A_{22} & A_{26} \\ A_{16} & A_{26} & A_{66} \end{bmatrix} \cdot \begin{Bmatrix} \varepsilon_{x0} \\ \varepsilon_{y0} \\ \gamma_{xy0} \end{Bmatrix} + \begin{bmatrix} B_{11} & B_{12} & B_{16} \\ B_{12} & B_{22} & B_{26} \\ B_{16} & B_{26} & B_{66} \end{bmatrix} \cdot \begin{Bmatrix} K_x \\ K_y \\ K_{xy} \end{Bmatrix} \quad (8)$$

Bending and torsional moments for M_x , M_y and M_{xy} unit length are given in equation 9.

$$\begin{Bmatrix} M_x \\ M_y \\ M_{xy} \end{Bmatrix} = \begin{bmatrix} B_{11} & B_{12} & B_{16} \\ B_{12} & B_{22} & B_{26} \\ B_{16} & B_{26} & B_{66} \end{bmatrix} \cdot \begin{Bmatrix} \varepsilon_{x0} \\ \varepsilon_{y0} \\ \gamma_{xy0} \end{Bmatrix} + \begin{bmatrix} D_{11} & D_{12} & D_{16} \\ D_{12} & D_{22} & D_{26} \\ D_{16} & D_{26} & D_{66} \end{bmatrix} \cdot \begin{Bmatrix} K_x \\ K_y \\ K_{xy} \end{Bmatrix} \quad (9)$$

The matrices $[A]$, $[B]$ and $[C]$ in the equations represent the axial/extension, coupling, and bending stiffness matrices.

$$A_{ij} = \sum_{k=1}^n [\bar{Q}_{ij}]_k (h_k - h_{k-1}), i=1,2,6 \text{ ve } j=1,2,6 \quad (10)$$

$$B_{ij} = \frac{1}{2} \sum_{k=1}^n [\bar{Q}_{ij}]_k (h_k^2 - h_{k-1}^2), i=1,2,6 \text{ ve } j=1,2,6 \quad (11)$$

$$D_{ij} = \frac{1}{3} \sum_{k=1}^n [\bar{Q}_{ij}]_k (h_k^3 - h_{k-1}^3), i=1,2,6 \text{ ve } j=1,2,6 \quad (12)$$

For symmetrical composite plates, the value $[B]$ is equal to zero. In this case, when equations 8 and 9 are arranged, equations 13 and 14 are obtained.

$$\begin{Bmatrix} N_x \\ N_y \\ N_{xy} \end{Bmatrix} = \begin{bmatrix} A_{11} & A_{12} & A_{16} \\ A_{12} & A_{22} & A_{26} \\ A_{16} & A_{26} & A_{66} \end{bmatrix} \cdot \begin{Bmatrix} \varepsilon_{x0} \\ \varepsilon_{y0} \\ \gamma_{xy0} \end{Bmatrix} \quad (13)$$

$$\begin{Bmatrix} M_x \\ M_y \\ M_{xy} \end{Bmatrix} = \begin{bmatrix} D_{11} & D_{12} & D_{16} \\ D_{12} & D_{22} & D_{26} \\ D_{16} & D_{26} & D_{66} \end{bmatrix} \cdot \begin{Bmatrix} K_x \\ K_y \\ K_{xy} \end{Bmatrix} \quad (14)$$

There is no coupling effect and no curvature due to axial loads and no normal deformations due to moments that occur in the mid-plane. Composite plates with various laying arrangements, which are of great importance according to the place they will be used, have different characteristics. These characteristics are known as symmetrical, equilibrium, angle fold, cross fold and semi-isotropic. The distance of both sides of the symmetrical sheet from the sheet midpoint should be equal. With symmetrical layer (0° , -45° , $+45^\circ$, 90° , 90° , $+45^\circ$, -45° , 0°) or simply (0° , -45° , $+45^\circ$, 90°) can be sampled. Opposite angles of $\theta=90^\circ$ and $\theta=0^\circ$ fiber angles are $\theta=0^\circ$ and $\theta=90^\circ$ degrees, respectively. There must be a plate with a certain material property, fiber direction and thickness of a layer in equilibrium and a separate plate within that composite layer with the same material properties and thicknesses, but with the opposite fiber direction. The equilibrium layer can be sampled with (90° , -45° , 0° , 45°) and (90° , 60° , 30° , -30° , 0° , -60°). In the angle layer composite plate, the fibers of each layer are located at angles $-\theta$ and θ . The angle can be exemplified by layer 2 (60° , -60° , 60° , -60°) or briefly (60° , -60°). In the cross layer composite layer, the fiber angles of each layer are $\theta=0^\circ$ and $\theta=90^\circ$. The cross layer can be sampled by layer (0° , 90° , 0° , 90°) or simply (0° , 90°). The fiber angles (θ) of the layers forming the semi-isotropic composite layer are at 0° , -45° , $+45^\circ$, 90° angles and are symmetrical. These layers also have a balancing feature. Semi-isotropic layer (0° , 90° , $+45^\circ$, -45°)s, (-45° , 90° , $+45^\circ$, 0°)s and (90° , -45° , 0° , $+45^\circ$)s [23,24,25,26,27].

2.2 Cover Design and Material

The composite cover has a width of 354 mm, a length of 1710 mm and a height of 234 mm. The composite valve consists of two combined structures, with and without ribs. The visual figure of the composite cover can be found in Figure 6.

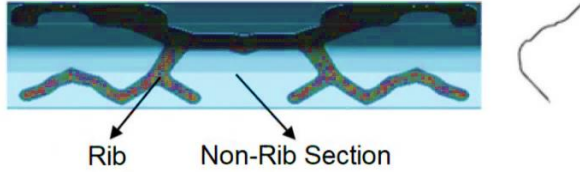


Figure 6. Ribbed and ribless portions of the composite door design

According to the usage conditions of the part, different laying angles were determined in each paving layer by using resin-impregnated unidirectional carbon fiber (prepreg) materials in order to reduce the effect of vibration loads on the part. Laying angle sequences were made using the rules in the literature under the main heading of design rules of layered composites. In this way, it is aimed to increase strength. The mechanical properties of the materials are given in Table 1.

Tablo 1. One way carbon/epoxy prepreg material properties

Parameter	Symbol	Carbon prepreg
Elasticity Module (0°)	GPa	121
Elasticity Module (90°)	GPa	8.6
Slip modulus	GPa	4.7
Poisson's ratio	-	0.27
Density	g/cc	1.49

The multi-layer composite plate is formed by overlapping orthotropic single-layer composite plates with different fiber directions in a symmetrical manner as in Figure 7. In the study, a composite cover design with 20 different laying angles was carried out.

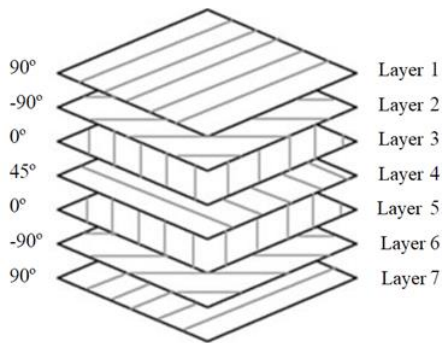


Figure 7. Composite material laying angles

2.2 Composite Orientation Angles

Fiber orientations angles, which is one of the design variables for the designed composite cover, are changed in each laying layer, and it is aimed to reduce the effect of vibration loads on the part according to the usage conditions of the part. Manufacturability was taken into account in determining the laying angles. Laying angles, which are frequently used in practice, were preferred for

layered composites in the study. The arrays with different orientation angles that make up the designs are given in Table 2. Laying sequences were modeled and analyzed with the ANSYS ACP module.

Table 2. Arrays with different orientation angles

Design no	Orientation angles
1	(45°, -45°, 45°, -45°, 45°, -45°, 45°)
2	(0°, 45°, -45°, 0°, -45°, 45°, 0°)
3	(0°, 45°, 90°, 0°, 90°, 45°, 0°)
4	(0°, 45°, 90°, 0°, -90°, -45°, 0°)
5	(-45°, 0°, 45°, 90°, 45°, 0°, -45°)
6	(45°, -45°, 45°, -45°, 45°, -45°, 45°)
7	(90°, -90°, 90°, -90°, 90°, -90°, 90°)
8	(45°, 90°, 45°, 90°, 45°, 90°, 45°)
9	(90°, -90°, 0°, 90°, 0°, -90°, 90°)
10	(90°, -90°, 45°, 90°, 45°, -90°, 90°)
11	(0°, -90°, 45°, 90°, 45°, 90°, 0°)
12	(90°, -90°, 0°, 0°, 0°, -90°, 90°)
13	(0°, 45°, 90°, 0°, 0°, -90°, 90°)
14	(90°, -90°, 45°, 90°, 0°, -90°, 90°)
15	(90°, -90°, 90°, 0°, 90°, -90°, 90°)
16	(45°, -45°, 0°, 0°, 0°, -45°, 45°)
17	(45°, -45°, 45°, 0°, 45°, -45°, 45°)
18	(45°, -45°, 0°, 45°, 0°, -45°, 45°)
19	(45°, -45°, 0°, 90°, 0°, -45°, 45°)
20	(90°, 0°, 90°, 0°, 90°, 0°, 90°)

3. Results and Discussion

All created designs were modeled and analyzed with the ANSYS ACP module. In the first column of the table, it gives the laying angles of the ribless section in the top row and the ribs in the bottom line. As a result of the analysis, mode 1, mode 2, mode 3, mode 4, mode 5 and mode 6 natural frequency values were obtained for each design. Obtained values are shown in Figure 8. Since the mode 1 natural frequency value is found to be zero for all designs, it is not included in the graph.

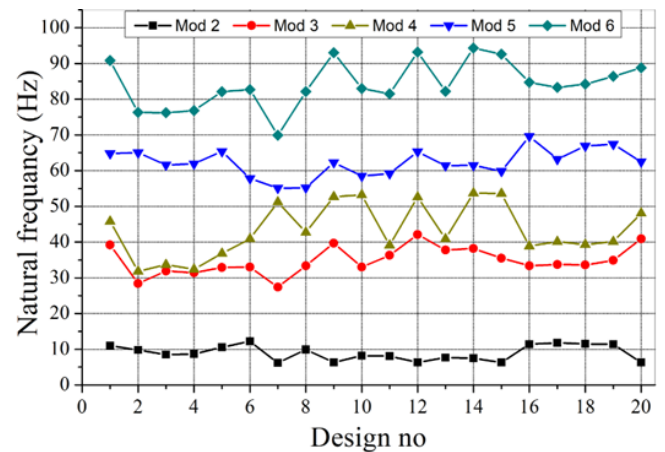


Figure 8. Natural frequency values in different laying sequences

When the analysis results were examined, it was seen that the best mode 2 natural frequency value of the structure was obtained in the 6th design. It is seen that this design has (45°, -45°, 45°, -45°, 45°, -45°, 45°).

45°, -45°, 45°) degree, angular and symmetrical arrangement. In this design, it was determined that mode 2 has 12.2 Hz, mode 3 33 Hz, mode 4 40.9 Hz, mode 5 57.8 Hz and mode 6 82.7 Hz natural frequency values. Good results were also obtained for the pavings made with 45°, -45° angles on the top and bottom layers and 0° angles in the center. The lowest mode 2 values were obtained with layer arrays with 0 and 90 degree laying angles. This result was reached with the natural frequency values obtained from designs 7, 9, 12, 15 and 20. When these results are evaluated, it is seen that it is possible to improve the mode 2 behavior of these and similar structures by designing the first layer by preferring 45°, -45° angle layers and symmetrical arrangement.

The best mode 3 natural frequency value of the structure was obtained with design number 12. This design is constituted by a layer arrangement with equilibrium conditional laying angles of (90°, -90°, 0°, 0°, 0°, -90°, 90°). The second design with a high mode 3 natural frequency value was determined as design number 20. This design has diagonal ply laying angles of (90°, 0°, 90°, 0°, 90°, 0°, 90°). It has been concluded that the lowest mode 3 values occur in layer arrays with 45 and 90 degree laying angles. These laying angles are available in designs 2, 3, 4, 6 and 7. When the results are evaluated, it is seen that it is possible to improve the mode 3 behavior of these and similar structures by designing 90° and 0° equilibrium arrays or 90° and 0° cross-floor pavements.

4. Conclusions

In the study, it was observed that with the increase of mode 2 and mode 3 natural frequency values, the other mode values increased. In this study, more focused on mode 2 and mode 3 natural frequency values, which are seen as critical for the structure. It has been concluded that the examined cover design gives the best mode 2 value (45°, -45°, 45°, -45°, 45°, -45°, 45°) if it has a degree, angular and symmetrical arrangement. In this design, mode 2 has a natural frequency value of 12.2 Hz, mode 3 33 Hz, mode 4 40.9 Hz, mode 5 57.8 Hz and mode 6 82.7 Hz. In this cover design, the best mode 3 natural frequency values (90°, -90°, 0°, 0°, 0°, -90°, 90°) degrees have been achieved with a layer arrangement with balance conditional laying angles. In this design, mode 3 has a natural frequency value of 6.3 Hz, mode 3 42.1 Hz, mode 4 52.6 Hz, mode 5 65.3 Hz and mode 6 93.2 Hz. It has been determined that in case the Mode 3 natural frequency value is aimed to be high (90°, 0°, 90°, 0°, 90°, 0°, 90°) it can be preferred in its structure with diagonal floor laying angles of 5°. In this design, it was determined that mode 3 has 6.3 Hz, mode 3 40.9 Hz, mode 4 48.1 Hz, mode 5 62.5 Hz and mode 6 88.8 Hz. The general results obtained in this study are given below.

- The best mode 2 behavior was obtained by choosing the 45°, -45 angle fold and symmetrical arrangement of the first layer in the laying arrangements.

- The lowest mode 2 values were obtained with layer arrays with 0 and 90 degree laying angles.

- The best mode 3 behavior is obtained by choosing the 90° and 0° balance arrays in the laying arrays.

- It has been observed that the mode 3 behavior gives close to the best value in case of 90° and 0° diagonal floor layings.

- It has been concluded that the lowest mode 3 values occur in layer arrays with 45 and 90 degree laying angles.

Conflict of Interest Statement

The authors declare that there is no conflict of interest in the study.

CRediT Author Statement

Mehmet Can Katmer: Conceptualization, Methodology, Software, Writing - original draft

Adnan Akkurt: Conceptualization, Supervision, Writing - original draft

Tolga Kocakulak: Writing - review & editing, Writing - original draft

References

1. Vo-Duy, T., Duong-Gia, D., Ho-Huu, V., Vu-Do, H. C., Nguyen-Thoi, T. (2017). Multi-objective optimization of laminated composite beam structures using NSGA-II algorithm. *Composite Structures*, 168, 498-509.
2. Ebrahimi, F., Nouraei, M., & Dabbagh, A. (2020). Modeling vibration behavior of embedded graphene-oxide powder-reinforced nanocomposite plates in thermal environment. *Mechanics Based Design of Structures and Machines*, 48(2), 217-240.
3. Solmaz, M. Y., Mustafa, Gür. Tabakalı Kompozit Plakalarda Takviye Malzemesi ve Oryantasyon Açısının Gerilme Analizine Etkisi. *Fırat Üniversitesi Doğu Araştırmaları Dergisi*, 6(1), 16-25.
4. Aydın, L., Artem, H. S., Savran, M. Genetik Algoritma Kullanılarak Boyutsal Kararlı Kompozit Malzemelerin Optimizasyonu. *Afyon Kocatepe Üniversitesi Fen Ve Mühendislik Bilimleri Dergisi*, 17(3), 1136-1145. DOI: 10.5578/fmbd.64041
5. Kaymaz, K., Zengin, B., Aşkın, M., Taşkaya, S. (2018). Investigation of Mechanical Stresses on Sandwich Composite Layers According to The Pressure By Making Use of Ansys Software. *Gümüşhane Üniversitesi Fen Bilimleri Enstitüsü Dergisi*, (CMES 2018 Sempozyum Ek sayısı), 79-93.
6. Küçükrendeci, İ. (2017). Nonlinear Vibration Analysis of Composite Plates on Elastic Foundations in Thermal Environments. *Afyon Kocatepe Üniversitesi Fen Ve Mühendislik Bilimleri Dergisi*, 17(2), 790-796. DOI: 10.5578/fmbd.57619
7. Karaman M., Öztürk E. (2021). Analysis of the Behavior of a Cross-Type Hydraulic Outrigger and Stabilizer Operating Under Determined Loads. *Engineering Perspective 1 (1): 22-29, 2021.* <http://dx.doi.org/10.29228/sciperspective.49248>
8. Turan, M. (2007). Tabakalı kompozit malzemelerde yüksek hızlı darbe hasarı. *Mühendis ve Makina*, 48(575), 3-8.
9. Saraçoğlu, M. H., & Gürlek, M. E. (2020). Tabakalı Kompozit Kirişlerin Eğilme Analizi. *Journal of Scientific Reports-B*, Number 1, 19-33, June 2020
10. Çevik, M. (2007). Basit mesnetli simetrik çapraz ve açılı tabakalı kompozit kirişlerin etkileşimli serbest titreşimleri. 15. Ulusal Mekanik Kongresi, 03-07 Eylül, Isparta.
11. Hüseyinoğlu, M., Tayfun, Abut. (2019). İki Ucu Ankastre U Çerçeve Yapının Modal Analizi. *Muş Alparslan Üniversitesi Fen Bilimleri Dergisi*, 7(2), 657-665. <https://doi.org/10.18586/msufbd.637678>
12. Yıldırım, Ş., Emir, E. S. İ. M. (2019). Çift Köprülülü Aski Tip Kren

- Sistemlerinin Sonlu Elemanlar Metodu ile Modal Analizi. Konya Mühendislik Bilimleri Dergisi, 7, 975-988.
13. Naskar, S., Mukhopadhyay, T., Sriramula, S., & Adhikari, S. (2017). Stochastic natural frequency analysis of damaged thin-walled laminated composite beams with uncertainty in micromechanical properties. *Composite Structures*, 160, 312-334. DOI: 10.36306/konjes.627067
 14. Abualnour, M., Houari, M. S. A., Tounsi, A., & Mahmoud, S. R. (2018). A novel quasi-3D trigonometric plate theory for free vibration analysis of advanced composite plates. *Composite Structures*, 184, 688-697.
 15. Şakar, G., Yaman, M., Bolat, F. Ç. (2010). Bal peteği sandviç kompozit yapıların dinamik analizi. 2. Ulusal Tasarım İmalat ve Analiz Kongresi, 11-12 Kasım, Balıkesir, 531-540.
 16. Atlıhan, G. (2010). Süreksizlik bölgesine sahip tabakalı kompozit kirişlerin titreşim analizi, Doktora Tezi, Pamukkale Üniversitesi Fen Bilimleri Enstitüsü, Pamukkale.
 17. Gibson, R. F. (2000). Modal vibration response measurements for characterization of composite materials and structures. *Composites Science And Technology*, 60, 2769-2780. DOI: 10.1016/S0266-3538(00)00092-0
 18. Yesilyurt, I., Gursoy, H. (2015). Estimation of elastic and modal parameters in composites using vibration analysis. *Journal of Vibration and Control*, 21(3), 509-524. DOI: 10.1177/1077546313486275
 19. Soni, P. J. and Iyengar, N. G. R. (1983). Optimal design of clamped laminated composite plates. *Fibre Science and Technology*, 19 (4), 281-296.
 20. Vatangül, E. (2008). Kompozit malzemelerin mekanik özelliklerinin belirlenmesi ve ansys 10 programı ile ısı gerilme analizi, Bitirme Projesi, Dokuz Eylül Üniversitesi Mühendislik Fakültesi Makine Mühendisliği Bölümü, İzmir.
 21. Baba, A. B. (2013). Delaminasyonlu tabakalı kompozit plakaların burkulma analizi, Yüksek Lisans Tezi, Dokuz Eylül Üniversitesi Fen Bilimleri Enstitüsü, İzmir.
 22. Kaw, A. K. (2005). *Mechanics of composite materials* (Second edition). USA: CRC Press.
 23. İnal, O., Balıkoğlu, F., & Ataş, A. (2018). Bolted joints in quasi-unidirectional glass-fibre NCF composite laminates. *Composite Structures*, 183, 536-544.
 24. Inal, O & Atas, A 2018, 'Experimental investigation of pinned joints in NCF Glass-Fibre reinforced composite plates', *Journal Of The Faculty Of Engineering And Architecture Of Gazi University*, vol. 33, no. 4, pp. 1445-1457. <https://doi.org/10.17341/gazimmfd.416441>
 25. Kiani, Y. (2017). Free vibration of carbon nanotube reinforced composite plate on point supports using Lagrangian multipliers. *Mechanica*, 52(6), 1353-1367. DOI 10.1007/s11012-016-0466-3
 26. Zhai, Y., Liang, S. (2017). Optimal lay-ups to maximize loss factor of cross-ply composite plate. *Composite Structures*, 168, 597-607. <http://dx.doi.org/10.1016/j.compstruct.2017.01.019>
 27. Shao, D., Hu, F., Wang, Q., Pang, F., & Hu, S. (2016). Transient response analysis of cross-ply composite laminated rectangular plates with general boundary restraints by the method of reverberation ray matrix. *Composite Structures*, 152, 168-182. <http://dx.doi.org/10.1016/j.compstruct.2016.05.035>